



Thermodynamic properties of SrAl₁₂O₁₉ and SrAl₄O₇

K. T. Jacob^{1,*} and Varun Shreyas¹

¹Department of Materials Engineering, Indian Institute of Science, Bengaluru 560012, India

Received: 23 June 2017

Accepted: 23 September 2017

Published online:
4 October 2017

© Springer Science+Business
Media, LLC 2017

ABSTRACT

Strontium aluminates are important compounds with interesting properties such as long-duration phosphorescence and elastically-deformation luminescence. They have potential application in flexible light emitting panels. Since there are serious discrepancies in available thermodynamic data for these compounds, a re-determination of their Gibbs energies of formation was undertaken using solid-state electrochemical cells incorporating single-crystal SrF₂ as the electrolyte in the temperature range from 1000 to 1300 K. However, the measurements were restricted to SrAl₁₂O₁₉ and SrAl₄O₇ because of the formation of strontium oxyfluoride phase between SrAl₂O₄ and SrF₂. For the reactions, SrO + 6 Al₂O₃ → SrAl₁₂O₁₉, $\Delta G^\circ/\text{J mol}^{-1} (\pm 280) = -83386 - 25.744 (T/\text{K})$, and SrO + 2Al₂O₃ → SrAl₄O₇, $\Delta G^\circ/\text{J mol}^{-1} (\pm 240) = -80187 - 25.376 (T/\text{K})$. The high entropy of SrAl₄O₇ and SrAl₁₂O₁₉ can be partly related to their complex structures. The results of this study are consistent with calorimetric data on enthalpy of formation of other Sr-rich aluminates and indicate only marginal stability for SrAl₄O₇ relative to its neighbours, SrAl₁₂O₁₉ and SrAl₂O₄. The thermodynamic data explain the difficulty in direct synthesis of phase pure SrAl₄O₇ and the formation of SrAl₂O₄ as the initial ternary phase when reacting SrO and Al₂O₃ or crystallizing from amorphous state, irrespective of composition.

Introduction

Tertiary oxides belonging to the system SrO–Al₂O₃ are useful in a variety of applications, most prominently in phosphors. The stable compounds in this system are, Sr₄Al₂O₇, Sr₃Al₂O₆, SrAl₂O₄, SrAl₄O₇ and SrAl₁₂O₁₉; Sr₄Al₂O₇ is stable only above 1403 K [1]. Two important metastable phases are Sr₄Al₁₄O₂₅ [2] and Sr₁₂Al₁₄O₃₃ [3, 4]. Monoclinic α-SrAl₂O₄ is unique among strontium aluminates in exhibiting elastically-deformation luminescence which is useful

for developing mechano-optical devices [5]. Long-duration phosphorescence has been achieved in Eu²⁺ and Dy³⁺ co-doped SrAl₄O₇ and SrAl₁₂O₁₉ [6]. Organic–inorganic flexible light emitting panels can be made from polystyrene and doped strontium aluminate [7]. Pr³⁺-activated SrAl₁₂O₁₉ shows photon-cascade emission with the quantum efficiency greater than 100% under vacuum ultraviolet excitation [8].

Thermodynamic data for SrAl₂O₄ are available in thermodynamic compilations [9, 10]. Ye et al. [11]

Address correspondence to E-mail: katob@materials.iisc.ernet.in

have estimated thermodynamic data for strontium aluminates by comparison with similar compounds and consistent with the phase diagram for the system SrO–Al₂O₃. The data for SrAl₂O₄ from the three sources [9–11] differ greatly as shown in Fig. 1. The enthalpy of formation of SrAl₂O₄, Sr₃Al₂O₆ and Sr₄Al₂O₇ from their binary oxides has been measured by Brisi et al. [12]. The chemical potential of SrO corresponding to a mixture of Sr₃Al₂O₆ and SrAl₂O₄ was measured by Levitski and Scolis [13] in the temperature range from 1150 to 1375 K using an electrochemical cell incorporating SrF₂ as the solid electrolyte. Gibbs energy of formation of SrAl₁₂O₁₉ was measured by Akolis et al. [14] in the temperature range from 1245 to 1380 K using an electrochemical cell. More recently, Ueda et al. [15] have reported the standard Gibbs energies of formation of SrAl₄O₇ and SrAl₁₂O₁₉ at 1723 K. They equilibrated oxide mixtures with liquid copper contained in a graphite crucible under CO gas atmosphere and measured the equilibrium concentration of strontium in liquid copper. Result of Ueda et al. [15] for SrAl₁₂O₁₉ differs significantly from the extrapolated data of Akolis et al. [14] and estimate of Ye et al. [11] as shown in Fig. 2. The inconsistency in available thermodynamic data on strontium aluminates prompted a redetermination. The most convenient method for measuring Gibbs energies of formation of strontium aluminates at high temperature is the use of solid-state electrochemical cells incorporating SrF₂ as the

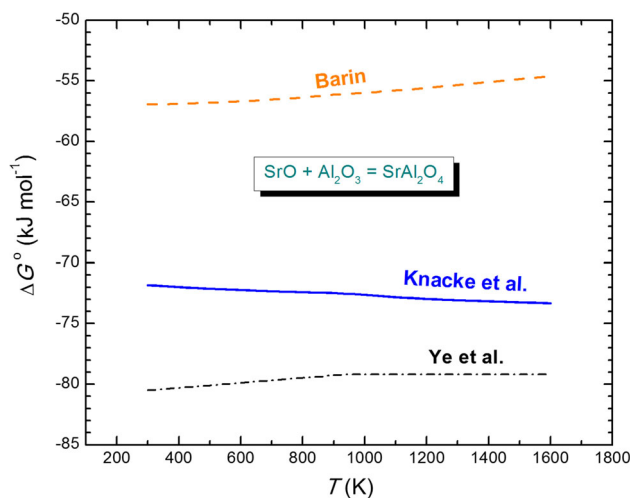


Figure 1 Temperature dependence of Gibbs energy of formation of SrAl₂O₄ from the literature: Barin [10] (orange dashed line); Knacke et al. [9] (blue solid line); Ye et al. [11] (black dash-dot line).

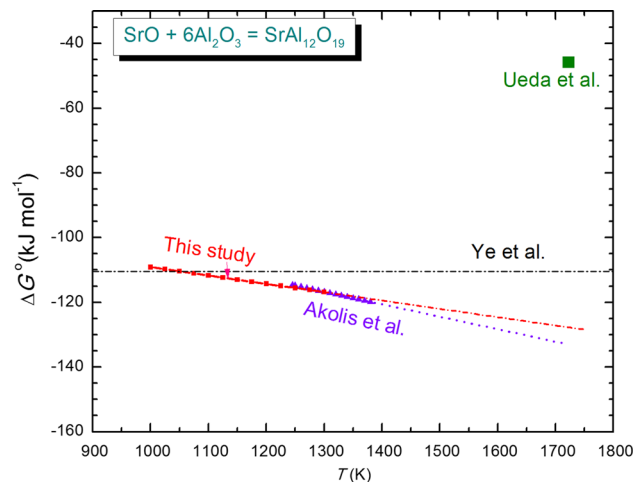


Figure 2 Comparison of Gibbs energy of formation of SrAl₁₂O₁₉ from its constituent binary oxides: Akolis et al. [14] (violet line); Ueda et al. [15] (olive square); Ye et al. [11] (black dash-dot line); this study (red line).

electrolyte. However, in preliminary experiments in this study cells containing SrAl₂O₄ at the electrode registered time-dependent electromotive force (EMF) suggesting secondary reactions related to the formation of a strontium oxyfluoride phase between SrAl₂O₄ and SrF₂. Hence, the measurements were restricted to SrAl₁₂O₁₉ and SrAl₄O₇.

SrAl₁₂O₁₉ crystallizes in the hexagonal system with a magnetoplumbite-type structure, space group P63/mmc (194) [16]. The structure has been characterized by ²⁷Al MAS and MQMAS solid-state NMR. There are five different Al sites; three octahedrally coordinated, one tetrahedrally coordinated, and one having fivefold coordination [17]. Each Sr atom is coordinated by twelve oxygen atoms forming an anticuboctahedron. The crystal structure of SrAl₄O₇ is monoclinic, space group C12/c1 (15) with four formula units in the unit cell. All the aluminium atoms are tetrahedrally coordinated [18]. Each Sr atom is coordinated by seven oxygen atoms forming a pentagonal bipyramid.

Materials and methods

Materials

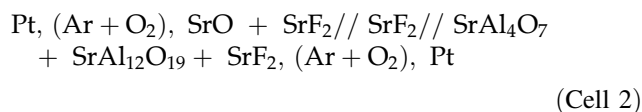
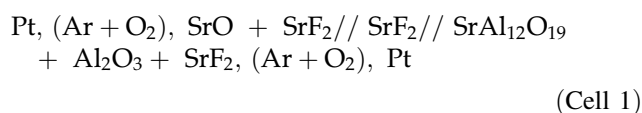
Aluminium nitrate nonahydrate (Al(NO₃)₃·9H₂O) and strontium nitrate (Sr(NO₃)₂), both of 99.995% purity on the basis trace metal analysis, obtained from Sigma-Aldrich were used as starting materials.

Two strontium aluminates, $\text{SrAl}_{12}\text{O}_{19}$ and SrAl_4O_7 , were prepared by spray drying a mixture of nitrates in the appropriate molar ratio. To decompose the nitrates, the dry powders were heated at $\sim 0.1 \text{ K s}^{-1}$ to 1073 K. The resulting products were amorphous. The powders were then ground in agate mortar and subsequently heat treated for crystallization at 1823 K. XRD confirmed the formation of phase pure aluminates. XRD pattern for white $\text{SrAl}_{12}\text{O}_{19}$ was almost identical to that in ICSD file number 01-080-1195. The hexagonal lattice parameters calculated from the ten major peaks are $a = b = 0.5569 \text{ nm}$ and $c = 2.2012 \text{ nm}$. XRD pattern for SrAl_4O_7 was very close to that in ICSD file number 01-072-1252. The lattice parameters of the monoclinic crystal structure, calculated using the ten major peaks are $a = 1.304 \text{ nm}$, $b = 0.9011 \text{ nm}$, $c = 0.5536 \text{ nm}$ and $\beta = 106.24^\circ$. Transparent single crystals of SrF_2 in the form of disc, 1.5 cm in diameter and 0.3 cm thick, were used as the solid electrolyte.

High-purity premixed ($\text{Ar} + \text{O}_2$) gas from a cylinder with oxygen partial pressure (P_{O_2}/P°) = 0.0276 was used in this study. It was first passed through columns containing sodium hydroxide to remove traces of CO_2 . The gas was then dried by passing through columns containing silica gel and anhydrous magnesium perchlorate and over boats containing phosphorous pentoxide.

Apparatus and procedure

The electromotive force (EMF) of the following solid-state electrochemical cells was measured as a function of temperature from 1000 to 1300 K.



Since Pt forms ternary oxides with SrO at higher oxygen pressures, a gas mixture with reduced oxygen partial pressure was employed. The reference electrode pellet was prepared by heating a compacted equimolar mixture of SrO and SrF_2 at 1300 K. The working electrodes were prepared in a similar manner by initially taking an equimolar mixture of SrF_2 and two neighbouring phases in the $\text{SrO-Al}_2\text{O}_3$

system ($\text{SrAl}_{12}\text{O}_{19} + \text{Al}_2\text{O}_3$ in Cell 1 and $\text{SrAl}_4\text{O}_7 + \text{SrAl}_{12}\text{O}_{19}$ in Cell 2). The presence of SrF_2 in each electrode was required to generate fluorine potential.

Since the apparatus used in this study for electrochemical measurements was similar to that described earlier [19, 20], only a brief description is given here. The electrode pellets were spring loaded on either side of a transparent SrF_2 single crystal. A Pt gauze attached to a Pt lead was inserted between each electrode and the electrolyte. A system of alumina tubes and rods was used to hold the pellets together under spring pressure. Platinum foils were used to prevent direct contact between electrode pellets and the alumina tubes or rods. The cell was assembled inside an outer alumina tube fitted with brass end caps, which had provision for gas inlet/outlet and electrical connections. The entire cell assembly was suspended inside a vertical resistance furnace with good temperature control ($\pm 1 \text{ K}$). The temperature of the cell was initially raised to 573 K. The moisture adsorbed on the ceramic tubes was removed by repeated evacuation of the outer alumina tube and refilling with dry premixed ($\text{Ar} + \text{O}_2$) gas of known composition from a cylinder. The oxygen partial pressure in the ($\text{Ar} + \text{O}_2$) mixture was (P_{O_2}/P°) = 0.0276, where $P^\circ = 1.013 \times 10^5 \text{ Pa}$ is the standard pressure. The same gas mixture was passed over both electrodes.

The EMF was measured using a digital voltmeter with the internal impedance greater than $10^{12} \Omega$ and sensitivity of 0.1 mV. To avoid the pickup of induced EMF on cell leads from furnace winding, a stainless steel foil was wrapped around the outer alumina tube and earthed. The time required to attain steady EMF varied from $\sim 40 \text{ ks}$ at the lowest temperature to $\sim 15 \text{ ks}$ at intermediary temperatures and $\sim 2 \text{ ks}$ at the highest temperature used in this study. To check reversibility small currents ($\sim 10 \mu\text{A}$) were passed in either direction through the cell and the EMF observed as a function of time. Gradual return of the EMF to the same value after successive displacements in opposite directions ensured electrochemical reversibility. The EMF was independent of the flow rate of ($\text{Ar} + \text{O}_2$) mixture through the cell from 1 to 5 mL s^{-1} . The flow rate during EMF measurements was maintained at 3 mL s^{-1} . Temperature cycling did not significantly affect the EMF. At the end of each experiment, the cell was dismantled after cooling and the electrodes were examined by optical

microscopy, XRD and SEM equipped with EDS. The phase compositions of all the electrodes of cells 1 and 2 were found to be unaltered by the high-temperature exposure. A summary of the characterization results is given in the supplementary file.

Results and discussion

The reversible EMF of the two cells was measured as a function of temperature in the range from 1000 to 1300 K. The results are summarized in Table 1 and displayed in Fig. 3.

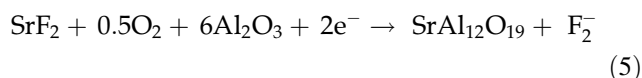
The EMF of both cells vary linearly with temperature. The least-mean square regression analysis gives,

$$E_1/\text{mV} (\pm 1.4) = 432.1 - 0.1334(T/\text{K}) \quad (3)$$

$$E_2/\text{mV} (\pm 1.7) = 407.2 - 0.1306(T/\text{K}) \quad (4)$$

where E_1 and E_2 refer to the EMF of cell 1 and cell 2, respectively. The uncertainties in Eqs. (3) and (4) are expanded uncertainties U (0.95 level of confidence) obtained by regression analysis. The EMF of the cells responds to the difference in the chemical potential of fluorine at the electrodes. In the range of fluorine potentials encountered in this study, SrF_2 is an ionic conductor with transport number of fluoride ions greater than 0.99.

The electrochemical reaction at the working electrode of cell 1 can be written as:



Corresponding reaction at the reference electrode of cell 1 is:

Table 1 EMF of cells 1 (SrO vs. $\text{SrAl}_{12}\text{O}_{19} + \text{Al}_2\text{O}_3$) and 2 (SrO vs. $\text{SrAl}_4\text{O}_7 + \text{SrAl}_{12}\text{O}_{19}$) as a function of temperature

T (K)	E_1 (mV)	E_2 (mV)
1000	564	535
1025	571	543
1050	573	546
1075	575	548
1100	577	549
1125	583	556
1150	587	556
1175	587	561
1200	593	565
1225	595	565
1250	598	571
1275	604	575
1300	605	576

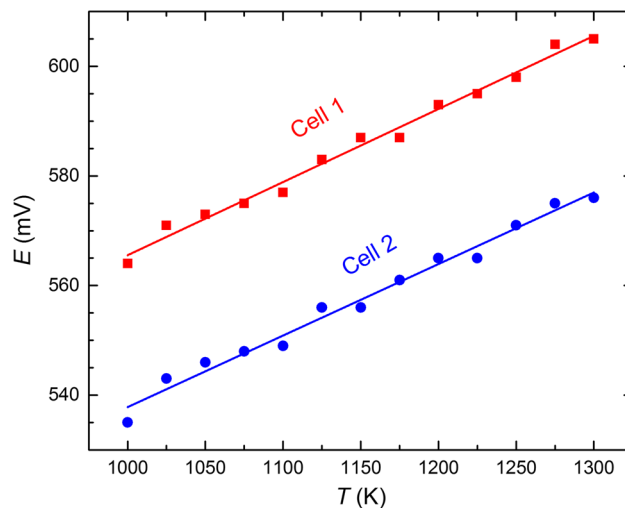
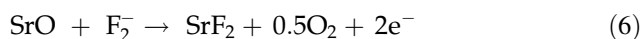
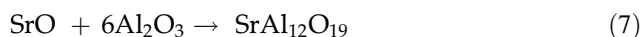


Figure 3 Temperature dependence of reversible EMF of the solid-state electrochemical cells: cell 1 (red filled square); cell 2 (blue filled circle).



For cell 1, virtual net reaction is:



From reversible EMF of cell 1, the standard Gibbs energy of formation of $\text{SrAl}_{12}\text{O}_{19}$ from its constituent binary oxides can be computed using the Nernst equation:

$$\begin{aligned} \Delta G^\circ/\text{J mol}^{-1}(\pm 280) &= -nFE \\ &= -83386 - 25.744(T/\text{K}) \quad (8) \end{aligned}$$

where $n = 2$ is the number of electrons involved in electrode reactions and $F = 96485.33289$ C/mol is the Faraday constant and E/V is the EMF. The first term on the right-hand side of Eq. (8) is the enthalpy of formation of $\text{SrAl}_{12}\text{O}_{19}$ from its constituent binary oxides ($-83.4 (\pm 0.95)$ kJ mol $^{-1}$) at the average experimental temperature of 1150 K. The second temperature-dependent term on the right-hand side of Eq. (8) with sign reversed gives the corresponding entropy change ($25.74 (\pm 0.82)$ J K $^{-1}$ mol $^{-1}$) for the reaction. The high entropy of $\text{SrAl}_{12}\text{O}_{19}$ relative to its component binary oxides may be related to statistical disorder of Al in AlO_5 polyhedra. Aluminium atoms in the trigonal bipyramid are axially displaced from the centre. The large number of binary oxide molecules (7) per formula unit of $\text{SrAl}_{12}\text{O}_{19}$ is another reason for the relatively large entropy value.

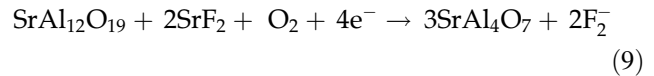
Assuming the applicability of Neumann-Kopp rule for the solid-state reaction (7), the standard enthalpy of formation of $\text{SrAl}_{12}\text{O}_{19}$ from its elements

at 298.15 K can be estimated as $\Delta H_f^\circ(298.15\text{ K}) = -10,729.6 (\pm 30) \text{ kJ mol}^{-1}$ by using the values of enthalpy of formation of Al_2O_3 ($-1675.69 (\pm 5) \text{ kJ mol}^{-1}$) and SrO ($-592.036 (\pm 3.8) \text{ kJ mol}^{-1}$) from thermodynamic data compilation of Knacke et al. [9]. Similarly, the standard entropy of $\text{SrAl}_{12}\text{O}_{19}$ at 298.15 K can be estimated as $S^\circ(298.15\text{ K}) = 387 (\pm 2.7) \text{ J K}^{-1} \text{ mol}^{-1}$ by using the values of $S_{\text{Al}_2\text{O}_3}^\circ$ ($50.949 (\pm 0.42) \text{ J K}^{-1} \text{ mol}^{-1}$) and S_{SrO}° ($55.522 (\pm 0.4) \text{ J K}^{-1} \text{ mol}^{-1}$) from thermodynamic data compilation of Knacke et al. [9]. However, because of the complicated crystal structure of $\text{SrAl}_{12}\text{O}_{19}$ with Al in three different coordination states, the application of Neumann–Kopp rule needs verification. Measurement of both high- and low-temperature heat capacity of $\text{SrAl}_{12}\text{O}_{19}$ is required to confirm and refine the data obtained in this study.

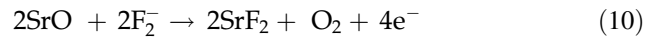
Gibbs energy of formation of $\text{SrAl}_{12}\text{O}_{19}$ from its constituent compounds obtained in this study is compared with values reported in the literature in Fig. 2. There is excellent agreement with the data of Akolis et al. [14] in the overlapping range of temperature, with a significant difference in the temperature dependence of Gibbs energy. Ye et al. [11] assume that entropy of formation from component binary oxides is zero. Although entropy change for solid-state reactions is generally small, they make a significant contribution to the stability of ternary oxides at high temperatures and should not be ignored. The result of Ueda et al. [15] at 1723 K is $\sim 82 \text{ kJ mol}^{-1}$ more positive than the extrapolated result of this study. In the successive experiments, Ueda et al. [15] equilibrated liquid Cu of unspecified purity with SrO , $\text{Al}_2\text{O}_3 + \text{SrAl}_{12}\text{O}_{19}$ and $\text{SrAl}_{12}\text{O}_{19} + \text{SrAl}_4\text{O}_7$ in a graphite crucible (99.9% pure) under flowing CO gas. The oxygen potential was assumed to be established by the equilibrium between graphite crucible and CO gas. From the equilibrium concentration of Sr in liquid Cu, they computed the Gibbs energy of formation of two strontium aluminates. The measured Sr concentrations in Cu were extremely low: 75.7 at. (atom) ppm when equilibrated with SrO , 3.14 at. ppm when equilibrated with $\text{Al}_2\text{O}_3 + \text{SrAl}_{12}\text{O}_{19}$ and 1.82 at. ppm when equilibrated with $\text{SrAl}_{12}\text{O}_{19} + \text{SrAl}_4\text{O}_7$. The results of this study suggest Sr concentrations in Cu more than 100 times lower than those reported by Ueda et al. [15], which are beyond the limit of quantitative measurement with ICP-AES. The higher

Sr concentrations reported by Ueda et al. [15] probably result from residual Sr impurities in Cu and Sr pickup from their graphite crucible.

The electrochemical reaction at the working electrode of cell 2 can be written as:



Corresponding reaction at the reference electrode of cell 2 is:



For cell 2, virtual net reaction is:



From the reversible emf of the cell, ΔG° for reaction (11) can be computed using the Nernst equation:

$$\Delta G^\circ / \text{J mol}^{-1} (\pm 660) = -157175 - 50.385 (T/\text{K}) \quad (12)$$

The value of n is 4 for this reaction. By combining Eqs. (7) and (11), the standard Gibbs energy of formation of SrAl_4O_7 from its constituent binary oxides is obtained:



$$\Delta G^\circ / \text{J mol}^{-1} (\pm 240) = -80187 - 25.376 (T/\text{K}) \quad (14)$$

The extrapolated result of this study is compared with the data of Ueda et al. [15] for SrAl_4O_7 at 1723 K in Fig. 4. The result from Ueda et al. [15] is $\sim 94 \text{ kJ mol}^{-1}$ more positive. The reason for the discrepancy in the data of Ueda et al. [15] has already been outlined in the discussion on $\text{SrAl}_{12}\text{O}_{19}$.

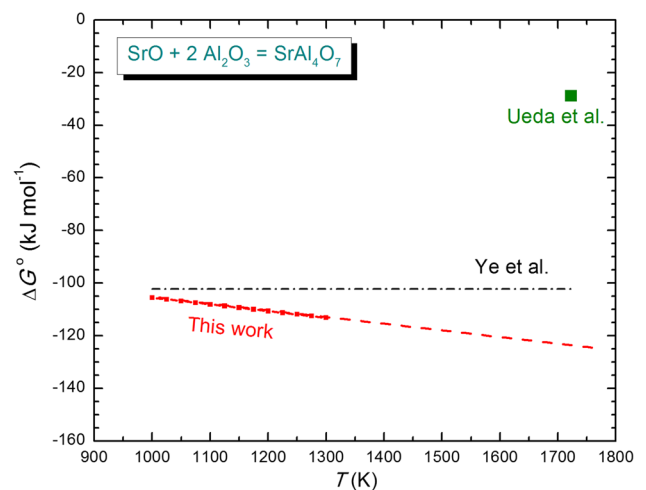


Figure 4 Comparison of Gibbs energy of formation of SrAl_4O_7 from its constituent binary oxides: this study (red line); Ueda et al. [14] (olive filled square); Ye et al. [11] (black dot-dash line).

According to Capron and Douy [21] $\text{SrAl}_{12}\text{O}_{19}$ is unstable above 1373 K; it decomposes to a mixture of $\text{Sr}_4\text{Al}_{14}\text{O}_{25}$ and $\text{SrAl}_{12}\text{O}_{19}$. The modified phase diagram suggested by Capron and Douy [21] is in violation of phase rule since four compounds are shown to coexist along a reaction isotherm at ~ 1335 K in the pseudo-binary $\text{SrO}-\text{Al}_2\text{O}_3$. Capron and Douy [21] suggest reappearance of SrAl_4O_7 as a stable phase above 1973 K. If the modified phase diagram Capron and Douy [21] is correct, Ueda et al. [15] should not have encountered SrAl_4O_7 at 1723 K. Further research is required to resolve this issue.

The second-law enthalpy of formation of SrAl_4O_7 from its constituent binary oxides is $(-80.2 \pm 1.1) \text{ kJ mol}^{-1}$ at the average experimental temperature of 1150 K. Corresponding second-law entropy change for this reaction is $(25.38 \pm 0.93) \text{ JK}^{-1} \text{ mol}^{-1}$. The high entropy of SrAl_4O_7 is probably related to rattling Sr in sevenfold coordination. Invoking Neumann–Kopp rule for reaction (13), the standard enthalpy of formation of SrAl_4O_7 from its elements at 298.15 K can be estimated as $\Delta H_f^\circ(298.15 \text{ K}) = -4023.6 (\pm 11) \text{ kJ mol}^{-1}$ using enthalpy of formation values for Al_2O_3 and SrO from Knacke et al. [9]. Similarly, using values of standard entropy of Al_2O_3 and SrO from Knacke et al. [9], the standard entropy of $\text{SrAl}_{12}\text{O}_{19}$ at 298.15 K can be estimated: $S^\circ(298.15 \text{ K}) = 182.8 (\pm 1.3) \text{ J K}^{-1} \text{ mol}^{-1}$. The high entropies of formation of $\text{SrAl}_{12}\text{O}_{19}$ and SrAl_4O_7 mirror similar properties of analogous calcium compounds $\text{CaAl}_{12}\text{O}_{19}$ and CaAl_4O_7 [22]. Calorimetric determination of enthalpy of formation and heat capacity as a function of temperature is required to confirm and refine the results of this study.

The enthalpy of mixing for the system $\text{SrO}-\text{Al}_2\text{O}_3$ is displayed in Fig. 5. The data for $\text{SrAl}_{12}\text{O}_{19}$ and SrAl_4O_7 are from this study, and data for SrAl_2O_4 , $\text{Sr}_3\text{Al}_2\text{O}_6$ and $\text{Sr}_4\text{Al}_2\text{O}_7$ are taken from Brisi et al. [12]. It is seen that the data obtained in the study integrate well with the calorimetric data of Brisi et al. [12] for strontium aluminates having higher concentration of SrO. Minimum enthalpy of mixing occurs at the equimolar composition. This is the reason for the appearance of SrAl_2O_4 as the first phase when reacting SrO and Al_2O_3 or crystallizing from the amorphous state, irrespective of composition. It is seen that the enthalpy of mixing for SrAl_4O_7 lies on a line connecting values for $\text{SrAl}_{12}\text{O}_{19}$ and SrAl_2O_4 . This explains the difficulty in synthesizing phase

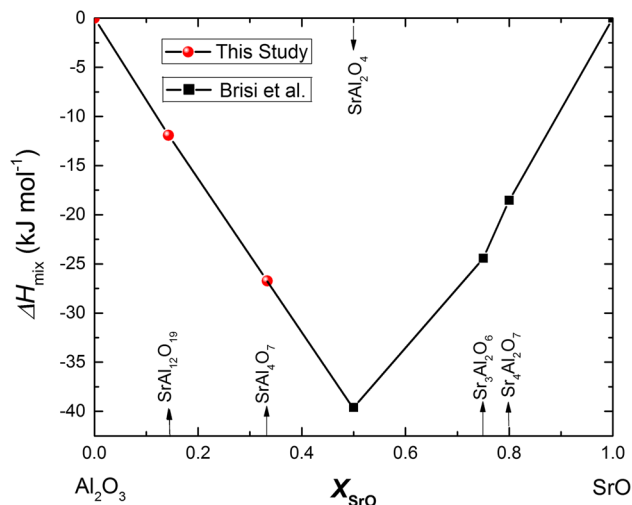
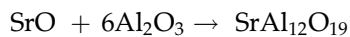


Figure 5 The enthalpy of mixing for the system $\text{SrO}-\text{Al}_2\text{O}_3$: this study (red filled circle); Brisi et al. [12] (black filled square).

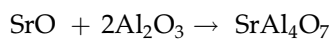
pure SrAl_4O_7 by direct solid-state reaction between SrO and Al_2O_3 . The instability of $\text{Sr}_4\text{Al}_2\text{O}_7$ at low temperatures (below 1403 K) is also revealed in Fig. 5. The compound is entropy stabilized.

Conclusion

In this study, the thermodynamic data for the compounds $\text{SrAl}_{12}\text{O}_{19}$ and SrAl_4O_7 have been determined by a potentiometric method. The standard Gibbs energies of formation for $\text{SrAl}_{12}\text{O}_{19}$ and SrAl_4O_7 in the temperature range 1000 to 1300 K are:



$$\Delta G^\circ / \text{J mol}^{-1} (\pm 280) = -83386 - 25.744 (T/\text{K})$$



$$\Delta G^\circ / \text{J mol}^{-1} (\pm 240) = -80187 - 25.376 (T/\text{K})$$

The apparent high entropy value of $\text{SrAl}_{12}\text{O}_{19}$ relative to its constituent binary oxides is caused by the large number of binary oxide molecules (7) per formula unit of $\text{SrAl}_{12}\text{O}_{19}$ and statistical disorder of Al in AlO_5 polyhedra. The high entropy of SrAl_4O_7 is probably related to rattling Sr atom having sevenfold coordination inside the pentagonal bipyramid. The standard enthalpies of formation of $\text{SrAl}_{12}\text{O}_{19}$ and SrAl_4O_7 from elements at 298.15 K, obtained by applying Neumann–Kopp rule, are $-10,729.6 (\pm 30) \text{ kJ mol}^{-1}$ and $-4023.6 (\pm 11) \text{ kJ mol}^{-1}$, respectively. Similarly, the standard or absolute entropies of $\text{SrAl}_{12}\text{O}_{19}$ and SrAl_4O_7 at 298.15 K are $387 (\pm 2.7)$

$\text{J K}^{-1} \text{mol}^{-1}$ and $183 (\pm 1.3) \text{ J K}^{-1} \text{mol}^{-1}$, respectively. These results can be confirmed and refined by calorimetric determination of enthalpy of formation and measurement of heat capacity as a function of temperature, starting at the lowest possible temperature. The minimum value of enthalpy of mixing at equiatomic composition explains the occurrence of SrAl_2O_4 as the first ternary oxide to form when SrO and Al_2O_3 are reacted at high temperatures irrespective of their relative concentrations.

Acknowledgements

One of the authors (KTJ) is grateful to the National Academy of Sciences, India (NASI), for the award of Platinum Jubilee Senior Scientist Fellowship. This research did not receive any specific grant from funding agencies in the public, commercial or not-for-profit sectors.

Compliance with ethical standards

Conflict of interest The authors declare that they have no conflict of interest.

Electronic supplementary material: The online version of this article (doi:[10.1007/s10853-017-1634-0](https://doi.org/10.1007/s10853-017-1634-0)) contains supplementary material, which is available to authorized users.

References

- Gantis F, Chemekova TY, Udalof YP (1979) The system $\text{SrO-Al}_2\text{O}_3$. *Russ J Inorg Chem* 24:260–263
- Yamaguchi O, Narai A, Shimizu K (1986) New compound in the system $\text{SrO-Al}_2\text{O}_3$. *J Am Ceram Soc* 69:C36–C37
- Wang M, Wang D, Lu G (1998) Research on fluorescence spectra and structure of single-phase $4\text{SrO}\cdot 7\text{Al}_2\text{O}_3\cdot \text{Eu}^{2+}$ phosphor prepared by solid-state reaction method. *Mater Sci Eng, B* 57:18–23
- Lin Y, Tang Z, Zhang Z (2001) Preparation of long-afterglow $\text{Sr}_4\text{Al}_{14}\text{O}_{25}$ -based luminescent material and its optical properties. *Mater Lett* 51:14–18
- Xu C, Yamada H, Wang X, Zheng X (2004) Strong elastoluminescence from monoclinic-structure SrAl_2O_4 . *Appl Phys Lett* 84(16):3040
- Katsumata T, Sasajima K, Nabae T, Komuro S, Morikawa T (1998) Characteristics of strontium aluminate crystals used for long-duration phosphors. *J Am Ceram Soc* 81(2):413–416
- Guo Y, Huang YM (2010) Green aluminate phosphors used for information display. *Key Eng Mater* 428–429:421–425
- Srivastava AM, Beers WW (1997) Luminescence of Pr^{3+} in SrAl_2O_4 : observation of two photon luminescence in oxide lattice. *J Lumin* 71:285–290
- Knacke O, Kubaschewski O, Hesselmann K (1991) Thermochemical properties of inorg. substances, 2nd edn. Springer, Berlin
- Barin I (1995) Thermochemical data of pure substances, 3rd edn. VCH, Weinheim
- Ye X, Zhuang W, Wang J, Yuan W, Qiao Z (2007) Thermodynamic description of $\text{SrO-Al}_2\text{O}_3$ system and comparison with other systems. *J Phase Equilib Diffus* 28:362–368
- Brisi C, Abbattista F (1960) Searches on the heats of formation of the strontium aluminated one. *Ann Chimica* 50:165–169 in Italian
- Levitski VA, Scolis YY (1974) Thermodynamics of double oxides I. Galvanic-cell study of strontium tungstates and aluminates. *J Chem Thermodyn* 6:1181–1190
- Akolis YY, Vintonyak VM, Levitskii VA, Yanishevskii VM (1983) Investigation of the thermodynamic properties of $\text{SrAl}_{12}\text{O}_{19}$ at the elevated temperatures by the emf method. *Inorg Mater* 19:228
- Ueda S, Utagawa K, Yamaguchi K (2008) Activity coefficient of strontium in liquid copper and the standard free energy of formation for $\text{SrO}\cdot 6\text{Al}_2\text{O}_3$ and $\text{SrO}\cdot 2\text{Al}_2\text{O}_3$. *Mater Trans* 49(6):1338–1341
- Lindop AJ, Matthews C, Goodwin DW, Haan JW, Ven JM, Kentgens APM, Nachtegaal GH (1975) The refined structure of $\text{SrO}\cdot 6\text{Al}_2\text{O}_3$. *Acta Cryst B* 31:2940
- Jansen SR, Hintzen HT, Metselaar R (1998) Multiple quantum ^{27}Al magic-angle-spinning nuclear magnetic resonance spectroscopic study of $\text{SrAl}_{12}\text{O}_{19}$: identification of a ^{27}Al resonance from a well-defined AlO_5 site. *J Phys Chem B* 102:5969–5976
- Lindop AJ, Goodwin DW (1972) The refined structure of $\text{SrO}\cdot 2\text{Al}_2\text{O}_3$. *Acta Cryst B* 28:2625
- Jacob KT, Hajra JP (1987) Measurements of Gibbs energies of formation of CoF_2 and MnF_2 using a new composite dispersed solid electrolyte. *Bull Mater Sci* 9:37–46
- Jacob KT, Abraham KP, Ramachandran S (1990) Gibbs energies of formation of intermetallic phases in the systems Pt-Mg , Pt-Ca , and Pt-Ba and some applications. *Metall Trans B* 21B:521–527

- [21] Capron M, Douy A (2002) Strontium dialuminate SrAl_4O_7 : synthesis and stability. *J Am Ceram Soc* 85:3036–3040
- [22] Allibert M, Chatillon C, Jacob KT, Lourtau R (1981) Mass-spectroscopic and electrochemical studies of thermodynamic properties of liquid and solid phases in the system $\text{CaO}-\text{Al}_2\text{O}_3$. *J Am Ceram Soc* 64:307–314